A TD-MFIE for a Vertically-Polarized Pulse Propagation over Irregular Terrains

Rodrigo B. V. Teperino and Fernando J. S. Moreira

Universidade Federal de Minas Gerais, Depto. Engenharia Eletrônica

Av Pres. Antônio Carlos 6627, Pampulha, Belo Horizonte, MG, CEP 31270-901

Abstract— **A time domain magnetic field integral equation (TD-MFIE) is developed and applied in the study of the propagation mechanisms of a vertically polarized electromagnetic pulse over an irregular ground. The atmosphere is assumed homogeneous and the conductivity of ground sufficiently small so to consider such ground a perfect magnetic conductor (PMC) for a vertical polarization. Furthermore, the terrain profile is assumed electrically smooth, such that back scattering is neglected and a forward scheme applied to obtain the surface magnetic currents of the equivalent problem, togheter with a marching-on-in-time (MOIT) technique to account for the time-varying characteristics.**

Keywords— **Ultra wideband radiowave propagation, time domain integral equation.**

I. Introduction

With the development of faster computers, the application of integral equations in the electromagnetic characterization of radiowave propagation has become attractive. In the frequency domain, efficient techniques based on the electric field integral equation (EFIE) and magnetic field integral equation (MFIE), have been developed and validated for VHF and UHF links over irregular terrains [1], [2], [3], [4], [5], [6], [7], [8]. In these works, the terrain is assumed to be electrically smooth and the atmosphere homogeneous. Considering that the Fresnel ellipsoid is not laterally obstructed, the terrain is also assumed to be invariant in the direction perpendicular to the plane of incidence. If the link is sufficiently large, such that a near-grazing incidence can be assumed over the smooth terrain profile, and for a ground with a small conductivity (about 0.2 S/m or smaller), good predictions are obtained even assuming the ground surface to be a perfect conductor (electric for horizontal polarization and magnetic for vertical). In [1], numerical results were compared against measurements conducted in Denmark for a vertical polarization and frequencies between 144 MHz and 1.9 GHz. The mean value of erros was never above 6 dB, with a maximum standard deviation of 10 dB.

The technique developed by Hviid *et. al* in [1] accounts for the spherical nature of the incident wavefront, differing from the bidimensional approach in [2] and [3]. Using the stationary-phase method to asymptotically evaluate the integral along the direction perpendicular to the plane of incidence, Hviid *et. al* were able to reduce the surface integral equation into a line one. Also, assuming a negligible back scattering due to the terrain smoothness, the equivalent magnetic currents were recursively obtained via a forward scheme, avoiding the hassles of the usual full-matrix analysis of the method of moments (MoM).

In [4] and [5], a similar procedure was adopted to numerically solve the problem, but using a MFIE instead of an EFIE. The results demonstrated that the MFIE-based technique provides the same level of accuracy but with a smaller number of basis functions to represent the equivalent magnetic currents (segments as long as 2 wavelengths were used to represent the terrain profile). A combination between the EFIE and the MFIE was further employed to account for terrain losses, by means of an impedance boundary condition [6]. Finally, the fast far-field approximation (FAFFA) developed in [2] to accelerate the integral equation solution was suited in [8] to the formulation in [4],[5].

The increasing interest in ultra wideband applications [9] has motivated the attainment of a time domain integral equation to characterize the propagation of electromagnetic pulses over irregular terrains. The MFIE was chosen, as it seems to be more appropriate than the EFIE for the problem discussed above. To achieve this goal, concepts and properties of the Fourier transform were applied into the MFIE formulation developed in [4],[5] for the frequency domain. So, as the transform operates just upon functions of time and the present boundary conditions are time-independent, all geometrical characteristics and properties used in advantage of a simpler formulation in [4],[5] are still retained and inerently accounted for. Also, the formulation in [4],[5] has a simple inverse Fourier transform, and the disadvantage is the appearance of a convolution integral in the resulting time domain MFIE (TD-MFIE). The TD-MFIE is then evaluated by applying the forward-scheme to recursively obtain the magnetic currents at a discrete number of points over the terrain profile. At each one of these points a marching-on-in-time (MOIT) scheme [10] is employed to obtain the time variation of the associate magnetic current.

Due to the computational burdem, only simple and relatively small problems are investigate: a PMC wedge-like profile and two consecutive ones. The results are compared against those provided by to independent methods: the MFIE-based formulation of [4],[5], with the frequency-domain results transformed into the time domain with the help of an inverse fast-Fourier transform (IFFT), and the asymptotic time domain uniform theory of diffraction (TD-UTD) [11].

Rodrigo B. V. Teperino, teperino@uol.com.br, Fernando J. S. Moreira, fernando@eee.ufmg.br. This work was partially financed by CAPES and CNPq.

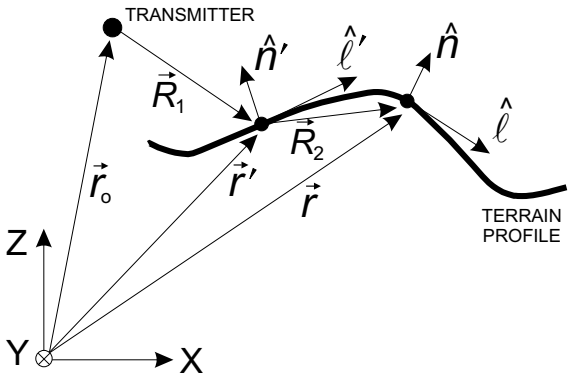

Fig. 1. Basic geometric parameters.

II. Frequency Domain MFIE

Before presenting the TD-MFIE, it is appropriate to conduct a briefly discussion on its frequency domain counterpart, which is used to establish the TD-MFIE after an inverse Fourier transformation. The MFIE is that developed and studied in [4],[5]. Basically, due to the assumptions briefly presented in Sect. I, for a near-grazing vertically-polarized incidence over a ground, this can be approximately treated as a perfect magnetic conductor (PMC). Assuming an homogeneous atmosphere (vacuum, for instance), the equivalence principle can be applied to substitute the present configuration by an equivalent problem with surface magnetic currents radiating in a free-space [12]. For this scenario, the necessary MFIE is written as [13]:

$$\hat{n} \times \vec{H}(\vec{r}) = 0 = \hat{n} \times \left[\vec{H}_{in}(\vec{r}) + \frac{1}{\eta}\, \vec{L}_1(\vec{M}) \right], \qquad (1)$$

where $\vec{H}_{in}$ is the phasor representation of the incident magnetic field radiated by the transmitting antenna, $\vec{M}$ is the phasor representation of the equivalent magnetic current (source of the scattered field in the equivalent problem), η is the free-space impedance ($\eta \approx 120\,\Omega$ for vacuum), $\hat{n}$ is the unit normal to the surface of ground at the observer's location (see Fig. 1), and

$$\vec{L}_1(\vec{M}) = -jk \oint_{S'} \left[\vec{M}(\vec{r}\,')\, G - \frac{1}{k^2} \nabla' \cdot \vec{M}(\vec{r}\,') \nabla' G \right] ds', \quad (2)$$

where S' denotes the domain of $\vec{M}$ and $k = 2\pi/\lambda = \omega/c$. In (2), G is the free-space Green's function, i.e.,

$$G = \frac{e^{-jk|\vec{r}-\vec{r}\,'|}}{4\pi \mid \vec{r} - \vec{r}\,' \mid}, \qquad (3)$$

where $\vec{r}$ and $\vec{r}\,'$ locate the observer and the equivalent source $\vec{M}$, respectively, both at S' (see Fig. 1).

Following the discussion in Sect. I, after the application of the stationary-phase method, the MFIE described in (1) is reduced into a line integral of the form [4],[5]:

$$\hat{n} \times \vec{H}_{in} = \frac{jk}{\eta} \int_{\ell'} [\hat{n} \times M(\ell')\hat{y}] \, \frac{e^{-jkR_2 - j\pi/4}}{4\pi \sqrt{\left(1 + \frac{R_2}{R_1}\right) \frac{R_2}{\lambda}}} \, d\ell', \quad (4)$$

where $\vec{R}_1$ and $\vec{R}_2$ are as in Fig. 1, $R_{1,2} = |\vec{R}_{1,2}|$, and, at the plane of incidence, $\vec{M} = \vec{M}(\ell') = M(\ell')\hat{y}$, where $\hat{y}$ is the unit normal to the plane of incidence. For the proper evaluation of the line integral in (4), it is convenient to define a locally-orthogonal coordinate system ($\hat{n}$, $\hat{\ell}$, $\hat{y}$, such that $\hat{n} \times \hat{\ell} = \hat{y}$ as in Fig. 1). Prime coordinates always refer to the source's location.

III. Time Domain MFIE

To obtain the desired TD-MFIE for the problem at hand, it is appropriate to apply an inverse Fourier transform on (4), as all the geometrical properties adopted to obtain (4) are not affected by such transform and, consequently, will remain effective in the time domain integral equation. Here, the adopted pair of Fourier transforms are [14]:

$$\mathcal{F}\{\mathcal{M}(t)\} = M(\omega) = \int_{-\infty}^{\infty} \mathcal{M}(t)\, e^{-j\omega t}\, dt\,, \qquad (5)$$

$$\mathcal{F}^{-1}\{M(\omega)\} = \mathcal{M}(t) = \frac{1}{2\pi} \int_{-\infty}^{\infty} M(\omega)\, e^{j\omega t}\, d\omega\,. \qquad (6)$$

Before applying the transform, it is appropriate to re-write (4) as

$$\hat{n} \times \vec{H}_{in} = \frac{-\hat{\ell}}{\eta} \int_{\ell'} jkM(\ell')\, G_{MM}(R_1, R_2)\, d\ell'\,, \qquad (7)$$

where

$$G_{MM}(R_1, R_2) = \frac{e^{-jkR_2 - j\pi/4}}{4\pi\sqrt{(1 + R_2/R_1)/(R_2/\lambda)}} \qquad (8)$$

can be interpreted as the magnetic Green's function of the MFIE after the application of the stationary-phase method in (1). Note that $-\hat{\ell} = \hat{n} \times \hat{y}$ does not depend on ℓ' and was taken out from the integral. So, applying (6) into (7) and with the help of the convolution theorem [14]:

$$\mathcal{F}^{-1}\left\{\hat{n} \times \vec{H}_{in}\right\} = \hat{n} \times \vec{\mathcal{H}}_{in}(t)$$
$$= \frac{-\hat{\ell}}{\eta} \int_{\ell'} \mathcal{F}^{-1}\{jkM(\ell')\} * \mathcal{F}^{-1}\{G_{MM}(R_1, R_2)\}\, d\ell'\,, \quad (9)$$

where $\vec{\mathcal{H}}_{in}$ is the actual incident magnetic field radiated by the antenna (i.e., in time domain). The first transform at the right-hand side of (9) is simply [14]

$$\mathcal{F}^{-1}\{jkM(\ell')\} = \frac{1}{c} \frac{\partial \mathcal{M}(\ell', t)}{\partial t}\,, \qquad (10)$$

while, for the second one,

$$\mathcal{F}^{-1}\{G_{MM}\} = \frac{(\sqrt{2\pi c})/(8\pi^2)}{\sqrt{R_2\left(1 + \frac{R_2}{R_1}\right)}} \int_{-\infty}^{\infty} \frac{e^{-jkR_2 + j\omega t}}{\sqrt{j\omega}}\, d\omega\,. \qquad (11)$$

The integral in (11) is evaluated in closed form [15]:

$$\int_{-\infty}^{\infty} \frac{e^{-jkR_2 + j\omega t}}{\sqrt{j\omega}}\, d\omega = \sqrt{\frac{\pi}{\tau}}\, \left[1 + \mathrm{Sign}\,(\tau)\right], \qquad (12)$$

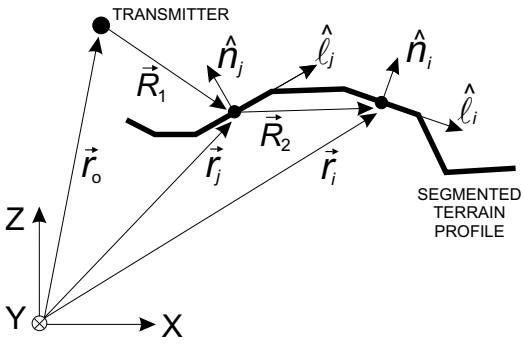

Fig. 2. Segmented terrain profile.

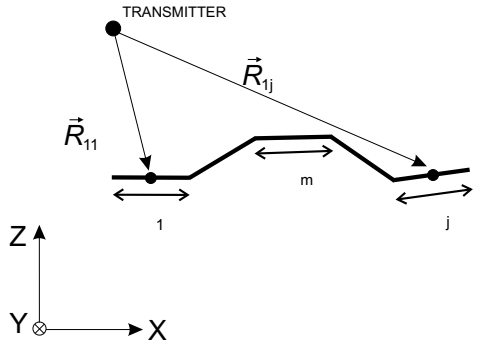

Fig. 3. Auxiliary geometry for the definition of the limits of the convolution integral.

where the time delay

$$\tau = t - \frac{R_2}{c} \tag{13}$$

and

$$\mathrm{Sign}(\tau) = \begin{cases} 1\,, & \text{for } \tau > 0 \\ 0\,, & \text{for } \tau = 0 \\ -1\,, & \text{for } \tau < 0 \end{cases} . \tag{14}$$

As $\tau > 0$ due to causality, (12) can be written as

$$\int_{-\infty}^{\infty} \frac{e^{-jkR_2+j\omega t}}{\sqrt{j\omega}}\, d\omega = 2\sqrt{\frac{\pi}{\tau}}\,. \tag{15}$$

Finally, substituting (10)–(15) into (9) and observing the causality principle:

$$\hat{n} \times \vec{\mathcal{H}}_{in}(t) = \frac{-\hat{\ell}}{4\pi\eta c} \int_{\ell'} \sqrt{\frac{2c}{R_2\,(1 + R_2/R_1)}} \times \int_{-\infty}^{\tau} \frac{\partial \mathcal{M}(\ell', t')}{\partial t'} \left(\frac{1}{\sqrt{\tau - t'}} \right) dt'\, d\ell' \,. \tag{16}$$

IV. Numerical Evaluation of the TD-MFIE

The numerical solution of the line integral in (16) is basically conducted as in [4],[5], i.e., the terrain profile is represented by straight segments (see Fig. 2) and $\mathcal{M}$ is assumed constant over the corresponding segment, with the associate geometric parameters taken at the segment's middle point. Any geometric parameter associated to the source will be stressed by the index "j" (see Fig. 2). Point-matching is adopted for the proper MoM solution, with the corresponding weighting delta function applied at the middle of the observation segment and oriented in the $\hat{\ell}_i$-direction. Any parameter corresponding to the observation point will be indicated by the index "i" (see Fig. 2). So, for a given observer at $\ell = \ell_i$, at a certain time $t = t_p$, and after the application of point-matching and the ractangle-rule to evaluate the line integral over the length Δ_j of the source segment, (16) is rewritten as

$$\hat{y} \cdot \vec{\mathcal{H}}_{in}(\ell_i, t_p) = \frac{1}{4\pi\eta c} \sum_{j=1}^{i} \left[\Delta_j \sqrt{\frac{2c}{R_2(1 + R_2/R_1)}} \times \int_{-\infty}^{\tau_p} \frac{d\mathcal{M}_j(t')}{dt'} \left(\frac{1}{\sqrt{\tau_p - t'}} \right) dt' \right], \tag{17}$$

where τ_p is that of (13) with $t = t_p$ and $\mathcal{M}_j(t')$ represents the unknown time variation of $\mathcal{M}$ at $\ell' = \ell_j$. In (17), it should be stressed that the summation goes from $j = 1$ up to i (with $i \geq j$) as back scattering is being neglected. Being N_b the number of segments over the terrain profile, N_b equations similar to (17) are established, one for each segment's middle point ($i = 1, \ldots, N_b$) and for a given $t = t_p$. This feature tremendously simplify the numerical solution, as a given $\mathcal{M}_i(t_p)$ can be directly obtained from the contributions of previously calculated currents, whose characteristics have already been stored for future use.

The MOIT goes as follows. To obtain a certain $\mathcal{M}_i(t)$, $t = t_p$ is varied from t_{ini} (the time when the transmitter is turned on) to the end of a given time window, set by the time when the last current ($i = N_b$) turns off. For each pair (ℓ_i, t_p), the contributions from $\mathcal{M}_j$ are calculated with j sequentially varied from 1 to i. Finally, for each j, the convolution integral in (17) must be numerically evaluated. Special care must be taken for the particular case where $j = i$ and $t' = t = t_p$.

We proceed with the numerical evaluation of the convolution integral. First, one should observe that $\mathcal{M}_j$ only exists during a certain time window $[t_{ini,\,j}, t_{end,\,j}]$. Thus, to avoid unnecessary calculations and memory storage, the limits of the convolution integral must be judiciously chosen. $\mathcal{M}_j$ is turned on at $t_{ini,\,j}$, when the incident wavefront radiated by the transmitter arrives at ℓ_j. So,

$$t_{ini,\,j} = t_{ini} + R_{1j}/c\,, \tag{18}$$

where R_{1j} is the distance between the transmitter and the center of segment j (see Fig. 3). While the incident wavefront continues its way down, $\mathcal{M}_j$ is kept turned on by the wavefronts radiated from the previous currents. So, with the help of Fig. 3, $t_{end,\,j}$ can be overestimated by the time that the incident wavefront takes to arrive at the middle of the first segment (R_{11}/c) plus the time taken to go from the middle of the first segment to the middle of the last one, along the terrain profile:

$$t_{end,\,j} = t_{end} + \left(R_{11} + \frac{\Delta_1}{2} + \sum_{m=2}^{j-1} \Delta_m + \frac{\Delta_j}{2} \right) \frac{1}{c}\,, \tag{19}$$

where t_{end} is the time when the antenna is turned off. Consequently, the lower limit of the convolution integral in (17)

should be set equal to $t_{ini,\,j}$ and such integral must not be initialized until $\tau_p \geq t_{ini,\,j}$. For the upper limit, it remains equal to τ_p while $\tau_p \leq t_{end,\,j}$ and set equal to $t_{end,\,j}$ after that condition is violated.

For the proper evaluation, the convolution integral (17) is expanded as:

$$\int_{t_{ini,\,j}}^{T_u} \frac{d\mathcal{M}_j}{dt'} \, \frac{dt'}{\sqrt{\tau_p - t'}} = \sum_{q=1}^{Q_j} \int_{t_{q-1}}^{t_q} \frac{d\mathcal{M}_j}{dt'} \, \frac{dt'}{\sqrt{\tau_p - t'}} \,, \quad (20)$$

where $T_u = \min(\tau_p, t_{end,\,j})$, $t_q = t_{ini,\,j} + q\,\Delta t_j$, and Δt_j set such that $t_{Q_j} = T_u$. Furthermore, the time variation of $\mathcal{M}_j$ is assumed linear in this work. So, for t' between t_{q-1} and t_q,

$$\frac{d\mathcal{M}_j(t')}{dt'} = \frac{\mathcal{M}_{j,q} - \mathcal{M}_{j,q-1}}{\Delta t_j} \,, \quad (21)$$

where $\mathcal{M}_{j,q-1}$ and $\mathcal{M}_{j,q}$ are the unknown current amplitudes to be determined at the middle of segment j and at the time instants t_{q-1} and t_q, respectively. Consequently,

$$\int_{t_{q-1}}^{t_q} \frac{d\mathcal{M}_j}{dt'} \, \frac{dt'}{\sqrt{\tau_p - t'}} = \frac{2\,(\mathcal{M}_{j,q} - \mathcal{M}_{j,q-1})}{\Delta t_j} \left(\sqrt{\tau_p - t_{q-1}} - \sqrt{\tau_p - t_q}\right) \,, \quad (22)$$

where, from the causality principle, $\mathcal{M}_{j,0} = 0$. So, with the help of (22), (20) can be rewritten as

$$\int_{t_{ini,\,j}}^{T_u} \frac{d\mathcal{M}_j}{dt'} \, \frac{dt'}{\sqrt{\tau_p - t'}} = \sum_{q=1}^{Q_j - 1} \mathcal{M}_{j,q}\,(C_{p,j,q} - C_{p,j,q+1}) + \mathcal{M}_{j,Q_j}\, C_{p,j,Q_j} \,, \quad (23)$$

where

$$C_{p,j,q} = \frac{2\,(\sqrt{\tau_p - t_{q-1}} - \sqrt{\tau_p - t_q})}{\Delta t_j} \,. \quad (24)$$

Substituting (23) back into (17):

$$\hat{y} \cdot \vec{\mathcal{H}}_{in}(\ell_i, t_p) = \frac{1}{4\pi\eta c} \sum_{j=1}^{i} \left\{ \Delta_j \sqrt{\frac{2c}{R_2(1 + R_2/R_1)}} \times \left[\sum_{q=1}^{Q_j - 1} \mathcal{M}_{j,q}(C_{p,j,q} - C_{p,j,q+1}) + \mathcal{M}_{j,Q_j} C_{p,j,Q_j} \right] \right\}, \quad (25)$$

which can be appropriately rewritten as

$$V_{i,p} = \sum_{j=1}^{i} \sum_{q=1}^{Q_j} \mathcal{M}_{j,q}\; Z_{i,p,j,q} \,, \quad (26)$$

where

$$\begin{aligned} V_{i,p} &= \eta\,[\hat{y} \cdot \vec{\mathcal{H}}_{in}(\ell_i, t_p)] \,, \\ Z_{i,p,j,q} &= \frac{\Delta_j}{4\pi c} \sqrt{\frac{2c}{R_2(1 + R_2/R_1)}}\,(C_{p,j,q} - C_{p,j,q+1}) \,, \\ Z_{i,p,j,Q_j} &= \frac{\Delta_j}{4\pi c} \sqrt{\frac{2c}{R_2(1 + R_2/R_1)}}\, C_{p,j,Q_j} \,. \end{aligned} \quad (27)$$

Note that the magnetic current $\mathcal{M}$ to be determined at the middle of segment i at $t = t_p$ is that where $j = i$ and $t_{Q_j} = t_{Q_i} = \tau_p = t_p$, (as for $i = j$, $R_2 = 0$). So, taking out $\mathcal{M}_{i,p}$ from the double summation in (26):

$$\mathcal{M}_{i,p} = \frac{1}{Z_{i,p,i,p}} \left(V_{i,p} - \sum_{\substack{\mathrm{j=1} \\ (j,q) \neq (i,Q_i)}}^{\mathrm{i}} \sum_{\mathrm{q=1}}^{\mathrm{Q_j}} \mathcal{M}_{j,q}\; Z_{i,p,j,q} \right) . \quad (28)$$

Caution should be taken to calculate $Z_{i,p,i,p}$ as $R_2 \to 0$. From (24) and (27), with $j = i$ and $t_{Q_i} = \tau_p = t_p$,

$$Z_{i,p,i,p} = \frac{\Delta_i}{4\pi c} \sqrt{\frac{2c}{R_2(1 + R_2/R_1)}} \left(\frac{2}{\sqrt{\Delta t_i}} \right), \quad (29)$$

which has numerical problems as $R_2 \to 0$. This just means that, in this situation, the rectangle-rule used to solve the line integral over the segment i is not appropriate. So, we must go back [just before (17)] and solve the integral with respect to ℓ' as $R_2 \to 0$:

$$\begin{aligned} Z_{i,p,i,Q_i} &= \lim_{R_2 \to 0} \frac{1}{4\pi c} \int_{\ell'} \sqrt{\frac{2c}{R_2(1 + R_2/R_1)}} \left(\frac{2}{\sqrt{\Delta t_i}} \right) d\ell' \\ &\approx \frac{\sqrt{2c}}{2\pi c \sqrt{\Delta t_i}} \int_{\ell'} \frac{d\ell'}{\sqrt{R_2}} = \frac{2}{\pi} \sqrt{\frac{\Delta_i}{c\,\Delta t_i}} \,, \end{aligned} \quad (30)$$

which must be used for $j = i$ and $t = \tau_p$ instead of (27).

A nested loop over i (in the outter loop) and t_p must then be conducted to calculate and store the several $\mathcal{M}_{i,p}$ given by the recursive use of (28). In this case, $t_p = t_{ini,\,i} + p\,\Delta t_i$, with $p = 1, \ldots, P_i$ and Δt_i set such that $t_{P_i} = t_{end,\,i}$. Finally, it must be stressed that both Δt_j and Δt_i, besides being established according to the conditions previously discussed, must not violate the stability condition $\Delta t \leq (\Delta\ell/c)$ for the proper convergence of the MOIT [10], where $\Delta\ell$ is the maximum segment length adopted in the discretization of the terrain profile.

V. Scattered Field

To establish the time domain electric field integral equation (TD-EFIE) necessary to obtain the electric field radiated by the equivalent currents, we start with the EFIE of [1]:

$$\vec{E}(\vec{r}) = \vec{E}_{in}(\vec{r}) - jk \int_{\ell'} (\hat{y} \times \hat{R}_2)\, M(\vec{r}\,') \times \left(1 + \frac{1}{jkR_2}\right) \frac{e^{-jkR_2 - j\pi/4}}{4\pi\sqrt{(1 + R_2/R_1)/(R_2/\lambda)}}\, d\ell' \,, \quad (31)$$

where now R_1 is the distance between the transmitter and the segment middle point and R_2 is the distance between this middle point and the receiver. So, applying (10) and (11) into (31), the TD-EFIE is given as:

$$\vec{\mathcal{E}}(\vec{r}, t) = \vec{\mathcal{E}_{in}}(\vec{r}, t) - \frac{1}{4\pi} \int_{\ell'} (\hat{y} \times \hat{R}_2) \sqrt{\frac{2c}{R_2(1 + R_2/R_1)}} \times \int_{t'} \left(\frac{1}{c} \frac{\partial \mathcal{M}}{\partial t'} + \frac{\mathcal{M}}{R_2} \right) \frac{1}{\sqrt{\tau - t'}}\; dt'\, d\ell' \,. \quad (32)$$

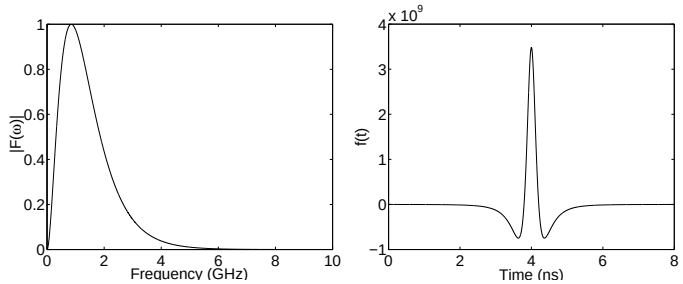

(a) (b)

Fig. 4. (a) Spectrum and (b) time variation of the excitation pulse.

VI. Numerical Results

Two simple problems are investigate: a PMC wedge-like profile and two consecutive ones. The results are compared against the frequency-domain MFIE of [4],[5], with the results transformed into the time domain with the help of an IFFT (MFIE+IFFT), and the TD-UTD developed in [11].

A. Excitation pulse

With excitation is the same one adopted in [11]. Its characteristics are depicted in Fig. 4 and can be described, in frequency domain, as:

$$F(\omega) = \frac{(P_1+P_2)^{(P_1+P_2)}}{P_1^{P_1}\, P_2^{P_2}} \left(1 - e^{-\omega T}\right)^{P_1} e^{-\omega P_2 T}\,, \quad (33)$$

here with $P_1 = 2$ and $P_2 = 1$. Its inverse Fourier transform is given by [11]:

$$f(t) = \mathrm{Re}\left[\frac{j}{\pi}\left(\frac{6,75}{t+jT} - \frac{13,5}{t+j2T} + \frac{6,75}{t+j3T}\right)\right]\,, \quad (34)$$

with $T = \log 3/(2\pi f_c)$ and $f_c = 850$ MHz.

B. Single PMC wedge

The single PMC wedge has a base of 200 m and height $h = 2$ m (see Fig. 5). The transmitter is located in the beginning of the wedge's profile at a height of 5 m. The receiver is placed at the end with height $h_R = 5$, 15, and 30 m.

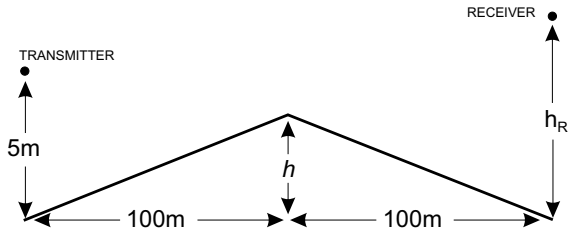

Fig. 5. Single PMC wedge profile.

For the MoM+IFFT analysis, a significant number of frequencies were adopted (up to 7 GHz as suggested by the spectrum of the incident pulse depicted in Fig. 4). The number of basis functions was varied for each frequency, such that the segments always had a length of about 2 wavelengths. For the TD-MFIE a spatial discretization of about 0.5 segments per wavelength was adopted, based on the highest significant frequency (7 GHz). The time discretization was determined by $\Delta t \approx 0.25$ ns.

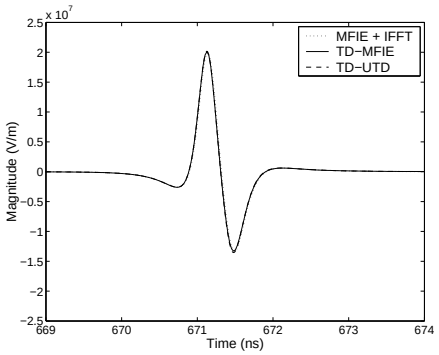

Fig. 6. Received electric pulse at $h_R = 5$ m over the wedge of Fig. 5.

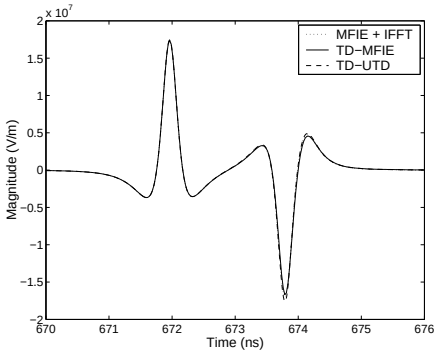

Fig. 7. Received electric pulse at $h_R = 15$ m over the wedge of Fig. 5.

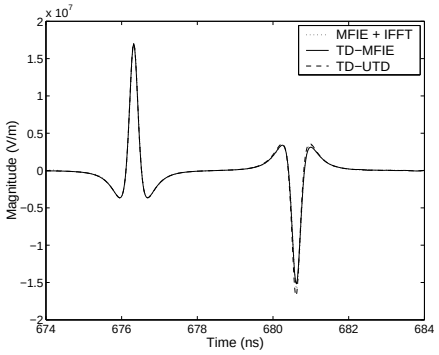

Fig. 8. Received electric pulse at $h_R = 30$ m over the wedge of Fig. 5.

The several results depicted in Figs. 6–8 present a good agreement. Small discrepancies are observed for the MFIE-based results with respect to the TD-UTD. For $h_R = 5$ m, Fig. 6 shows that the three techniques present basically the same result. For $h_R = 30$ m, shown in Fig. 8, the MFIE results present a slightly different magnitude and asymmetry with respect to the asymptotic TD-UTD.

C. Two consecutive PMC wedges

For the verification of the efficiency and accuracy of the methods, the propagation over two consecutive wedges was

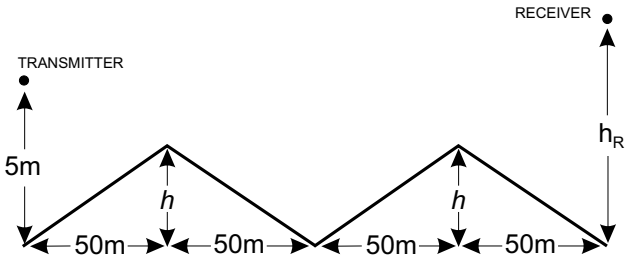

Fig. 9. Two consecutive wedges profile used in simulations

also considered (see Fig. 9). The main difference from the previous case is the presence of the double diffraction, which is not accounted for by the present TD-UTD [11]. So, only the results of the TD-MFIE and MFIE+IFFT are presented. Like in the previous single wedge, $h_R = 5$, 15, and 30 m and the respective scattering results are presented in Figs. 10–12. The same excitation, segmentation, and time discretization were odopted. Here, once more, one observes the good agreement between the TD-MFIE and the MFIE+IFFT.

VII. Conclusions

This work presented a time domain magnetic field integral equation (TD-MFIE) for the description of the propagation of a vertically-polarized electromagnetic pulse over an irregular ground. The numerical results were compared agianst the frequency domain MFIE, with the help of an IFFT, and the TD-UTD, presenting a good agreement.

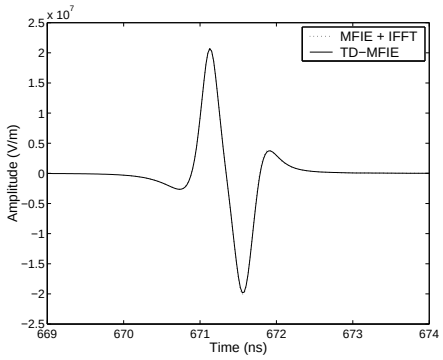

Fig. 10. Pulse in receiver with a height of $h_R = 5$ m over two consecutive perfect magnetic conductor wedges shown in Fig. 9.

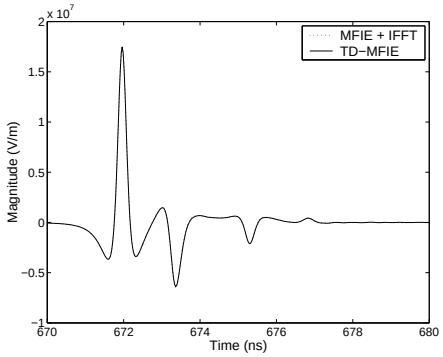

Fig. 11. Pulse in receiver with a height of $h_R = 15$ m over two consecutive perfect magnetic conductor wedges shown in Fig. 9.

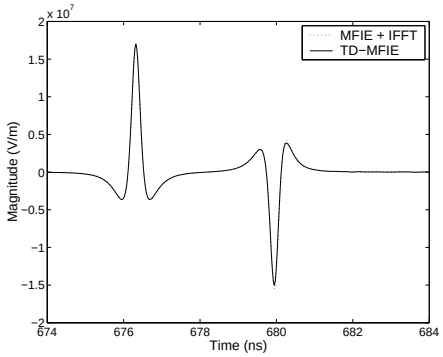

Fig. 12. Pulse in receiver with a height of $h_R = 30$ m over two consecutive perfect magnetic conductor wedges shown in Fig. 9.

References

[1] J. T. Hviid, J. B. Andersen, J. Toftgård, e J. Bøjer, "Terrain-based propagation model for rural area–an integral equation approach," *IEEE Trans. Antennas Propagat.*, vol. 43, pp. 41–46, Jan. 1995.

[2] C. Brennan e P. Cullen, "Application of the fast far field approximation to the computation of uhf pathloss over irregular terrain," *IEEE Trans. Antennas Propagat.*, vol. 46, no. 6, pp. 881–889, Jun. 1998.

[3] C. Brennan, P. Cullen, e L. Rossi, "An mfie-based tabulated interaction method for uhf terrain propagation problems," *IEEE Trans. Antennas Propagat.*, vol. 48, no. 6, pp. 1003–1005, Jun. 2000.

[4] F. J. S. Moreira, "Mfie-based propagation prediction," *2001 SBMO / IEEE MTT-S Int. Microw. Optoelect. Conference (IMOC'01)*, pp. 195–198, Aug. 2001.

[5] F. J. S. Moreira, "Mfie-based prediction for uhf vertically-polarized wave propagation over irregular terrains," *2001 IEEE APS Int.Symp. Digest*, vol. 1, pp. 456–459, Jul. 2001.

[6] F. J. S. Moreira, "Aplicação de equações integrais para a predição da propagação radioelétrica sobre solos suavemente irregulares e incidência rasante," *X Simp. Bras. Microondas e Optoeletrônica (SBMO 2002)*, pp. 191–195, Ago. 2002.

[7] A. E. Freitas, "Predição de cobertura em enlaces radioelétricos sobre terrenos irregulares através de equações integrais," *PPGEE-UFMG*, Ago. 2001.

[8] R. B. V. Teperino, "Aplicação do método faffa para a predição de propagação sobre terrenos suavemente irregulares," *V Cong. Bras. Eletromag. (CBMag2002)*, p. 25, Nov. 2002.

[9] K. Siwiak, "Ultra-wide band radio: A new pan and postioning technology," *IEEE Vehic. Tech. Society News*, Feb. 2002.

[10] G. Manara, A. Monorchio, e R. Reggiannini, "A space-time discretization criterion for a stable time-marching solution of the electric field integral equation," *IEEE Trans. Antennas Propagat.*, vol. 45, no. 3, pp. 527–532, Mar. 1997.

[11] K. L. Borges, "Caracterização banda-larga do canal rádio utilizando a teoria uniforme da difração no domínio do tempo (td-utd)," *PPGEE-UFMG*, Mar. 2003.

[12] R. F. Harrington, *Time-Harmonic Electromagnetic Fields*, McGraw Hill, New York, 1961.

[13] A. J. Poggio e E. K. Miller, *Computer Techniques for Electromagnetics*, Pergamon, Oxford, UK, 1973.

[14] R. N. Bracewell, *The Fourier Transform and its Applications*, McGraw Hill, New York, second edition, 1986.

[15] I. S. Gradshteyn e I. M. Ryzhik, *Table of Integrals, Series, and Products*, Academic Press, San Diego, CA, fourth edition, 1980.